INVESTIGATING THE ROUGHNESS EFFECT OF BIOFOULING ON PROPELLER PERFORMANCE

P. Kellett, K. Mizzi, Y. K. Demirel and O. Turan

Department of Naval Architecture, Ocean and Marine Engineering, University of Strathclyde, 100 Montrose Street, Glasgow G4 0LZ, UK, paula.kellett@strath.ac.uk

ABSTRACT

As a result of the increasing pressure being placed on the marine industry to address ship emissions, regulations to govern the fuel efficiency and efficient operation of ships in the form of the Energy Efficiency Design Index (EEDI) (IMO, 2014) and Energy Efficiency Operation Index (EEOI) (IMO, 2009a) have recently come into force. These have been introduced alongside regulations concerning specific emissions requirements (UNFCCC). Attention has therefore been turned to all aspects of ship design and operation which have impact on their efficiency. In turn, this paper focuses on the effects of biofouling on propeller surfaces highlighting the benefits of reducing biofouling. This subject was the focus of a recently completed EU-Funded FP7 Project entitled FOUL-X-SPEL (2011). This paper investigates the detrimental impacts of biofouling on the performance of a real ship propeller using Computational Fluid Dynamics (CFD) simulations. Initially, the CFD approach used in this study was validated through CFD open-water tests of a propeller. A previously-developed CFD approach for approximating the surface roughness that results from biofouling has then been applied in order to predict the effects on propeller efficiency. The roughness effects of a typical coating and different fouling conditions on the propeller performance were therefore predicted for various advance coefficients Results indicated negative effects of biofouling on the propeller efficiency and the importance of the mitigation of such effects, supporting the importance of informing the industry about the impacts such that they are able to make informed decisions regarding regular propeller maintenance and cleaning.

Keywords: Biofouling, CFD, Propeller Efficiency, Roughness, Open Water

1. INTRODUCTION

The recent introduction of regulatory legislation for ship emissions in the maritime industry has brought about the need for improving energy efficiency for environmental benefits. Although ships have been identified to be one of the most efficient mode of bulk transportation in terms of emissions per tonne of cargo carried, a study carried out by the International Maritime Organisation (IMO, 2009b) indicated the potential energy efficiency improvements that could be attained using technologies or operational methods. IMO's GHG study in 2007 reported shipping to emit around 1046 tonnes of greenhouse gases for that same year. This amounts to 3.3% of global emissions with 870 tonnes of it being carbon dioxide making this the most important gas emitted by ships. Although these numbers are near negligible, if not addressed accordingly, they are likely to increase drastically in the coming years. A projection outlined by Fang et al. (2013) indicated an increase of the world seaborne trade in the near future, predicting it to double by 2030. The increase of shipping volume will lead to an increase in ship emissions and IMO's second GHG study indicated that in the absence of policies, by the year 2050, ship emissions could multiply by a factor of around 2 to 3 times that of current levels. This therefore identifies a problematic issue, one that requires attention and recognition as a growing concern and the need for improving energy efficiency to minimise emissions from the shipping sector.

An Energy Efficiency Design Index (EEDI) (IMO, 2014) was therefore developed by a specialist group of the IMO known as the Marine Environmental Protection Committee (MEPC) as an incentive to control and lower Green House Gas emissions. The Designed EEDI of a vessel is estimated by calculating the predicted carbon emissions emitted compared to the useful work done by the ship (i.e. tonnes of cargo transported per nautical mile). EEDI restriction values assigned by the IMO differ by ship type and size. EEDI regulations were enforced on the 1st January 2013 and a phased implementation plan will see the restrictions become more stringent over the years. Ambitions to improve energy efficiency in vessel operations are commonly shared with ship owners

seeking to cut down fuel costs and expenses. The total ship transportation cost breakdown has changed significantly in recent years. Prior to 2008, the initial capital expenditure of a vessel was the main cost when compared to the operational and bunker cost throughout a ship's lifetime. With operating costs maintaining a constant rate throughout the years and bunker prices increasing significantly, the fuel costs of a vessel are becoming more significant. Hence, with the continuous increase of fuel costs, a vessel's fuel consumption has become a ship owner's prime concern which leads directly to considering the energy efficiency of the vessel (Hansen and Dinham-Peren, 2014).

Ship energy consumption depends on the performance of different components of the ship system; one significant component being the ships' hydrodynamic system comprising hull resistance, propulsion efficiency and hull-propeller interaction. These aspects can be address in a number or ways, both in terms of design and operation. For instance, studies (Kawamura et al., 2012, Hansen et al., 2011, Patience and Atlar, Schuiling, 2013) suggest that the installation of Energy Saving Devices (ESD) on a ship can result in a significant improvement in energy efficiency. From an operational perspective, marine biofouling is an increasing problem from both economic and environmental points of view in terms of increased resistance, increased fuel consumption, increased GHG emissions and transportation of harmful non-indigenous species (NIS). It should be kept in mind that even a small amount of fouling may lead to a significant increase in fuel consumption. Due to its negative effects on ship efficiency and the marine environment, it is very desirable to mitigate the accumulation of biofouling on ship hulls. While improving the energy efficiency of existing ships retrofitted with new antifouling paints, it is equally important to accurately model and understand the potential effects of biofouling on ship resistance and to demonstrate the importance of the mitigation of such effects by carrying out scientific research. However, at present, there is no complete method available to predict the effect of biofouling on ship frictional resistance. The ITTC (2011b) therefore recommends researchers to develop new formulae or methods, using experimental data, for the prediction of the effects of coatings and biofouling on ship resistance. With the increased availability of computational power and advances in numerical tools and modelling software, the use of numerical procedures are becoming more popular in aiding to maximise the energy efficiency saving potential.

This paper introduces a developed numerical design parametric approach with the aim to analyse the impact of marine fouling on the propeller efficiency. The initial step of the investigation was to validate the general open water numerical simulation approach by comparing results with experimental values at model scale for a well-known benchmarking case, the Potsdam Propeller Test Case (PPTC). The same validated approach was then applied to a real propeller, again firstly in model scale. The numerical model was then modified to account for biofouling effects of different degrees in order to analyse the impact on propeller characteristics at full scale for the real propeller case. The results present the impact that different levels of fouling have on the thrust and torque coefficients and hence the open water efficiency of the propeller, at three different advance coefficients.

A case study is carried out in this paper for an in-service Coastal Tanker vessel. This vessel formed one of the focus vessels for the EU-Funded FP7 Project AQUO (Aquo Consortium, 2012). During the course of this project, a range of model scale tests were carried out using this vessel, as well as CFD simulations. These are presented in detail in (Aquo Consortium, 2014, 2015a). The main dimensions of the vessel are presented in Table 1:

Table 1: Main dimensions for coastal tanker.

Data	**Symbol**	**Full scale**	**Model scale**
Scale	λ [-]	-	20
Length Overall	L_{OA} [m]	124.5	6.225
Breadth Moulded	B [m]	18	0.9
Draught: Fore - Aft	T [m]	8.12 - 8.12	0.406 – 0.406
Propeller Type		CPP	CPP
Propeller Diameter	D [m]	4.8	0.24
Hub Diameter	D_H [m]	1.344	0.0672
Number of Blades	Z [-]	4	4
Skew	S_K [°]	33.5	33.5
Pitch Ratio at 0.7r/R	P/D [-]	0.87	0.87

Some details relating to this case study are also included in Aquo Consortium (2015b) where a discussion is made regarding potential underwater noise mitigation measures, and their expected impact not only on the underwater radiated noise performance of a vessel but also their impact on the vessels fuel efficiency. In particular, the impacts of hull and propeller cleaning are presented, and this measure is suggested to be beneficial for both noise and efficiency performance.

2. BACKGROUND

2.1 PROPULSION EFFICIENCY

Propeller designs are generally differentiated and compared by their thrust *(T)* and torque *(Q)* characteristics. These parameters are generally non-dimensionalised to thrust *(K_T)* and torque *(K_Q)* coefficients that are used to compute the propulsion efficiency *(η_o)*. These coefficients can then be plotted for a range of advance coefficients *(J)* producing propeller curves, from which the optimum efficiency and operating point of a propeller can be identified. Due to the nature of an open water test environment where the propeller is immersed and rotated in an isolated water environment with a constant uniform flow velocity *(V_A),* respective propeller curves are only able to demonstrate characteristics for uniform flow simulations. Once fitted behind a vessel, incoming flow from the stern, more technically known as the wake, is non-uniform, thus changing propeller performance. This being said, open water characteristics are necessary for the calculation of propeller efficiency (η_D) that is a function of open water efficiency (η_o), hull efficiency (1-t)/(1-w) and relative rotative efficiency (η_R) as can be seen in equation (1).

$$\eta_D = \frac{\eta_o (1-t) \eta_R}{(1-w)} \tag{1}$$

2.2 OPEN WATRER TESTS

Propeller performance is traditionally predicted by carrying out experimental open water tests at model scale which tends to be time consuming enabling a fewer designs to be analysed. They produce reliable results at model scale; however scaling issues are encountered when using extrapolation procedures. On the other hand, numerical simulation methods allow full sale analyses in various conditions with the option of analysing various designs simultaneously. Together with the advance in computational power, CFD has been developed to produce fairly accurate results and is an accepted means of investigation on the basis of validation and verification procedures. One common approach is to use numerical methods at the initial stages of ship design before moving onto more reliable experimental tests to validate the CFD results at model scale and carry out numerical investigation at full scale.

A number of numerical tools have been established and developed over the years to provide modern day state of the art technology. Most common numerical methods are Boundary Element Method (BEM) and Reynolds-Averaged Navier-Stokes (RANS) computations. Being an inviscid approach, BEM require less computational power but is incapable of capturing viscous effects. This was outlined by Hsin et al. (2009) claiming that the BEM is incapable of accurately capturing the viscous effects such as the boundary layer and flow separation, thus failing to properly predict the performance. This would also be particularly critical when investigating fouling on the propeller blades. On the other hand RANS methods are capable of simulating viscous effects and capturing flow details Bertram (2011). However, they require additional computational power and cost in contrast to BEM. The advance of technology, computational power and the continuous development of commercial CFD codes have enabled RANS simulations to be worthwhile and they are now considered to be the preferred numerical approach. Hybrid BEM-RANS methods have also been used for preliminary stages due to computational cost benefits

For good quality CFD RANS simulations, appropriate mesh refinements, choice of turbulent model and proper selection of physics are of prime importance. Nakisa et al. (2010) carried out a study investigating the different models and highlighted that the Shear Stress Transport (SST) k-ω turbulence model, together with a sliding mesh domain produced better results for this type of simulation giving an average error of 8% for KT, 13% for KQ and 11% for η_o when compared to experimental values. The author continues to add that the accuracy

decreased in extreme load conditions. These comments are further supported by Li's (Da-Qing, 2002) remarks indicating that the error difference between his experimental and numerical results for KT and KQ are 3% and 5% respectively within a certain range of J and with the error increasing outside these conditions. He further outlines that the mesh density had no significant effect on the propeller performance prediction, but it produces different results for local flow quantities. Li (Da-Qing, 2002) also outlines that KQ is generally over predicted and that error magnitudes are larger than those of KT. He reasons this behaviour as a lack of the transition model in the RANS solver. In model scale conditions, the boundary layer over the blade is rarely fully turbulent due to the low Reynolds number mostly resulting in laminar flow. Turbulent models that assume fully turbulent flow generate strong turbulent viscosity and shear stresses on the blade surfaces hence over predicting the skin coefficient resulting in an over predicted KQ and under predicted KT. This being said, Arikan et al. (2012) analysed a podded propeller in a similar manner that produced a greater error for thrust than torque that could be explained by the highly skewed propeller resulting in very little laminar flow.

Vladimir et al. (2009) indicates that the International Towing Tank Conference (ITTC) scaling methods are not accurate in predicting the Reynolds number effect at full scale. He studied the scale effects on propellers with different magnitudes of skew in turbulent flow. Results indicated that laminar regions on the blade are smaller for higher skew blades. It was concluded that the scale effects in open water models were found to be dependent on the blade geometry and the propeller load which could be explained by the variation in magnitude of pressure and friction components. In order to try to account for these additional errors in scaling model test results to full scale, the validation work in this paper, to validate the approach in general has been carried out in model scale. However to assess the impact of roughness in a more realistic case, the same approach has been applied to a real ship propeller, with both propeller and roughness simulated in full scale. Vladimir et al. (2009) also stated that the inaccuracy of CFD procedures is also due to the negligence of roughness effects which in general can be introduced as correction factors for full scale models. Nevertheless, it has recently been shown in (Demirel et al., 2014b, Demirel et al., 2013, 2014a) that the effect of surface roughness can be accurately simulated using modified wall functions in CFD software and that the effect of coatings and fouling can be investigated.

2.3 NUMERICAL PREDICTION OF THE EFFECT OF BIOFOULING ON FLOW

Granville (Granville, 1958, 1978) proposed a similarity law scaling procedure for the prediction of the effects of a particular surface roughness on the frictional resistance of any arbitrary body covered with the same roughness, utilising the experimentally obtained quantities. Grigson (1985) proposed a method which is partly experimental and partly theoretical, just like the ones proposed by Granville (Granville, 1958, 1978). When it comes to CFD-based models, there are fewer studies investigating the roughness effects of coatings and biofouling on ship resistance. Currently, physical modelling of the roughness sources, such as coatings or biofouling, in CFD is practically impossible due to their complex geometries. However, once the relation of $\Delta U^+ = f(k^+)$ is known, it can be employed in the wall-function or the turbulence models of the CFD software, as discussed by Patel (1998). The use of CFD-based unsteady RANS models is of vital importance, since the phenomenon can be simulated by means of a fully non-linear method.

Several studies exist which model the effects of a uniform sand-grain roughness either using wall-functions (e.g. Suga et al. (2006), Apsley (2007)) or using near-wall resolution (e.g. Krogstad (1991), Aupoix (2007)). Eça and Hoekstra (2011) showed that the effect of uniform sand-grain roughness on the frictional resistance of flat plates of full-scale ship lengths at full-scale ship speeds can be accurately simulated using either wall-functions or near-wall resolution. Khor and Xiao (2011) investigated the effects of fouling and two antifouling coatings on the drag of a foil and a submarine by employing a CFD method. They used the equivalent sand grain roughness height and the built-in wall-function which considers the uniform sand-grain roughness function model proposed by Cebeci and Bradshaw (1977), based on Nikuradse's data (1933). Castro et al. (2011) carried out unsteady RANS CFD simulations of a full-scale KCS model with hull roughness using wall-functions. However, they used a constant roughness function and roughness allowance formulation proposed by the ITTC (1990). Recently, Mizzi et al. (2014) proposed a CFD model for the frictional resistance prediction of antifouling coatings. Although it was shown that the effect of surface roughness can be modelled using modified wall function in CFD, the proposed roughness function model was only suitable for some of the marine coatings and rather simplistic.

3 NUMERICAL MODELLING

3.1 MATHEMATICAL FORMULATION

In this study a RANS approach was applied using the commercial CFD software Star-CCM+ version 9.0.2, which was developed by CD-Adapco. The super computer facility (ARCHIE-WeSt) at the University of Strathclyde was utilised to allow faster and more complex simulations. The numerical solver uses RANSE to solve the governing equations simulating a three-dimensional environment using the SST k-ω model assuming a fully turbulent flow. The governing equations were discretised using a Finite Volume Method and a SIMPLE algorithm was used to solve the velocity-pressure coupling. The SST k-ω model is a two-equation eddy-viscosity turbulence model that considers an additional non-conservative cross-diffusion term to the k-ω model. This modification enhances the capability of the model allowing it to produce similar results to that of the k-ε model, thus enabling the system to have a hybrid structure with the best of both worlds. This in turn, blends the ε approach in the far field and the ω model near the walls, making it suitable for adverse pressure gradients and separating flows (CD-Adapco, 2014). The propeller was submerged in an immersed incompressible water liquid environment of constant density and segregated flow represented by the continuity and momentum flow equations (Ferziger and Peric, 2002).

$$div\, v = 0 \tag{2}$$

$$\frac{\partial(u_i)}{\partial t} + div(u_i v) = div(\nu\, grad\, u_i) - \frac{1}{\rho} div(pi_i) + b_i \tag{3}$$

where, $\bar{u}_i$ is the average Cartesian component of the velocity vector and $\nu = \mu / \rho$ the kinematic viscosity.

3.2 PROPOSED CFD APPROACH FOR FOULING CONDITIONS

The velocity profile in the log-law region of the turbulent boundary layer can be defined by

$$U^+ = \frac{1}{\kappa}\ln(y^+) + B - \Delta U^+ \tag{4}$$

in which k is the von Karman constant, y^+ is the non-dimensional normal distance from the boundary, B is the smooth wall log-law intercept and ΔU^+ is the roughness function. By using Eq (4), one can represent the change in the velocity profile due to roughness using DU^+, and the velocity profile can be defined by simply subtracting ΔU^+ from the smooth velocity profile. It should be borne in mind that ΔU^+ simply vanishes in the case of a smooth condition. ΔU^+ values are typically obtained experimentally, since there is no universal roughness function model for every kind of roughness. Reference may be made to Jiménez (2004) for a comprehensive review on rough wall turbulent boundary layers.

Schultz and Flack (2007) determined the roughness functions for three dimensional rough surfaces similar to those used by Shockling et al. (2006). Schultz (2007) proposed that the roughness function behaviour of a range of fouling conditions follow the roughness functions of Schultz and Flack (2007) and Shockling et al. (2006), based on his previous work presented in Schultz (2004). This is a reasonable assumption, since the roughness functions of real surfaces are expected to show behaviour that is between the monotonic Colebrook and inflectional Nikuradse type roughness functions, such as those presented by Schultz and Flack (2007) and Shockling et al. (2006), as shown in Figure 1. In addition, Schultz (2007) presented the equivalent sand roughness heights for a range of coating and fouling conditions together with the NSTM (Naval Ships' Technical Manual) (Naval Ships' Technical Manual, 2002) rating and average coating roughness (Rt_{50}) based on his extensive experiments including Schultz (2004) (Table 2).In this paper's study, the roughness function values of Schultz and Flack (2007) shown in Figure 1 were used to develop a roughness function model to be employed in the CFD software to represent the coating and fouling conditions given by Schultz (2007), as shown in Table 2.

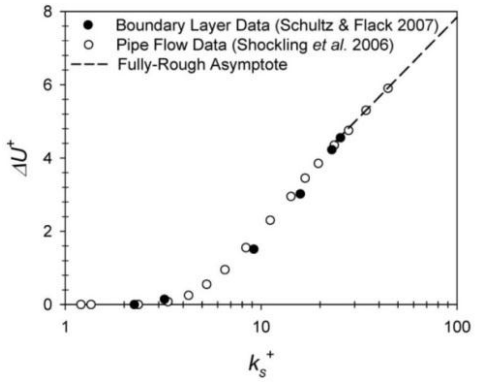

Figure 1: Roughness function vs. roughness Reynolds numbers (Schultz, 2007).

The present predictions were made based on the assumptions that the given fouling conditions can be represented by these roughness functions and roughness length scales. Schultz (2007) validated these assumptions and this method by comparing his results with other studies such as Hundley and Tate (1980) and Haslbeck and Bohlander (1992), documenting the effects of coatings and biofouling on ship powering through full-scale trials. An appropriate roughness function model was fitted to the roughness function values of Schultz and Flack (2007). This roughness function model is presented such that it is in the form of the built-in roughness function model of STAR-CCM+ for application convenience. Details of the proposed model can be found in Demirel et al. (2015).

Table 2: A range of representative coating and fouling conditions (Schultz, 2007).

Description of condition	NSTM rating*	k_s (mm)	Rt_{50} (mm)
Hydraulically smooth surface	0	0	0
Typical as applied AF coating	0	30	150
Deteriorated coating or light slime	10-20	100	300
Heavy slime	30	300	600
Small calcareous fouling or weed	40-60	1000	1000
Medium calcareous fouling	70-80	3000	3000
Heavy calcareous fouling	90-100	10000	10000

*NSTM (2002)

3.3 GEOMETRY AND BOUNDARY CONDITIONS

In order to accurately simulate the PPTC open water tests for validation, available geometry information allowed the modelling of the propeller and respective shaft. However, shaft geometry details were not provided for the real propeller case and thus not modelled which may account for some variations in the levels of accuracy obtained in the two different sets of model scale simulations when compared to experimental results. A velocity flow was specified for the inlet boundary condition and a pressure field for the outlet. The cylindrical boundary was set to a symmetry condition simulating the no-slip (wall) propeller in submerged water conditions.

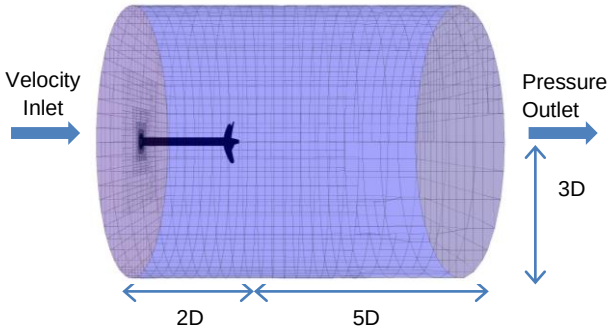

Figure 2: Boundary conditions

3.4 MESH GENERATION

There are various ways of simulating rotating propellers in CFD, in particular the Moving Reference Frame (MRF) method and the Rotating Mesh also known as the Sliding Mesh approach. For the prior, the domain rotates about an axis yielding transient calculations producing time-accurate results that require high computational power. For the MRF approach which is less computationally expensive, the domain remains stationary with an assigned frame of reference rotating about a pre-defined axis with respect to the global co-ordinate system. MRF simulations carry out a steady-state approximation to a transient problem producing time-averaged results. The latter method is less computationally demanding that provides sufficient accuracy (Kellet et al., 2013).

As discussed in (Mizzi et al., 2014), a negligible difference was produced between the two methods and thus the MRF approach was applied. However in this study, for the real propeller case a rotating mesh with sliding interface approach was adopted as the work was part of a larger study into underwater radiated noise prediction, where the sliding mesh approach is vital. Near-wall mesh generation must be performed with care since this is directly related to the roughness heights representing fouling conditions. The prism layer thickness and prism layer numbers were, therefore, determined such that y^+ is always higher than 30, and higher than k^+, as per CD-ADAPCO (2014)'s suggestion. Hence, the resulting y^+ values were very high as the k^+ values were high for most of the fouling conditions. It was also important to check the thickness of the first layer of cells within the prism layers at the propeller wall boundaries, to ensure that the modelled roughness was less than half that of this first layer. If the roughness is greater than the thickness of this first layer of cells, then it is approximated to be the same thickness as that layer and hence will make the results inaccurate.

4 RESULTS

4.1 VALIDATION STUDY

In order to validate the CFD approach applied to this study, the open water performance of the hydraulically smooth propeller with no added surface roughness was first simulated for the PPTC propeller in model scale. The open water test validation was taken from a previous study carried out on Propeller Boss Cap Fins (PBCF) optimisation analysis (Mizzi et al., 2014). These were carried out using an open source, model-scale, controllable pitch propeller in a pull test configuration, designed by (SVA) who provide the experimental open water test results allowing comparison and validation of our simulation model.

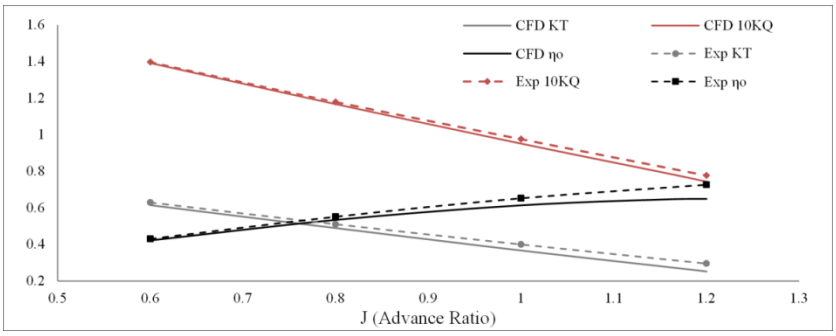

Figure 3: Comparison of experimental and predicted results for PPTC validation

The above graph (Figure 3) demonstrates the discrepancy between experimental and numerical results for the PPTC propeller open water characteristics. For advance coefficients between 0.6 and 1 J, numerical results yielded an open water efficiency accuracy of 4%. The graph indicates that the accuracy decreases significantly outside this range especially for higher values of J. This goes well in agreement with other author's findings explaining that this behaviour is a result of the lack of the transition model in the simulation. The RANS simulation for this study assumes a fully turbulent flow which in turn fails to predict the transition behaviour in the boundary layer. Hence, the error can be minimised by either employing a transition model into the simulation or by carrying out open water tests at full scale. For the latter, the transition region within the boundary layer is less significant compared to that for a model-scale, thus improving accuracy.

Secondly, the outlined approach was applied to the real propeller case, again in model scale. These results were compared to the model scale propeller open water test results generated by SSPA as outlined in Annex C of (Aquo Consortium, 2014). In these tests, the propeller rotation speed, n, was set to 15RPS / 900RPM to match the speed used in the model tests. The inlet velocity, V_A, was then varied to achieve the required advance coefficient, J. The water density in the simulations was also set to fresh water to match the conditions in the model tests. The figure below presents a comparison between the measured and predicted propeller thrust coefficient, K_T, torque coefficient,$10K_Q$, and open water efficiency, η_0.

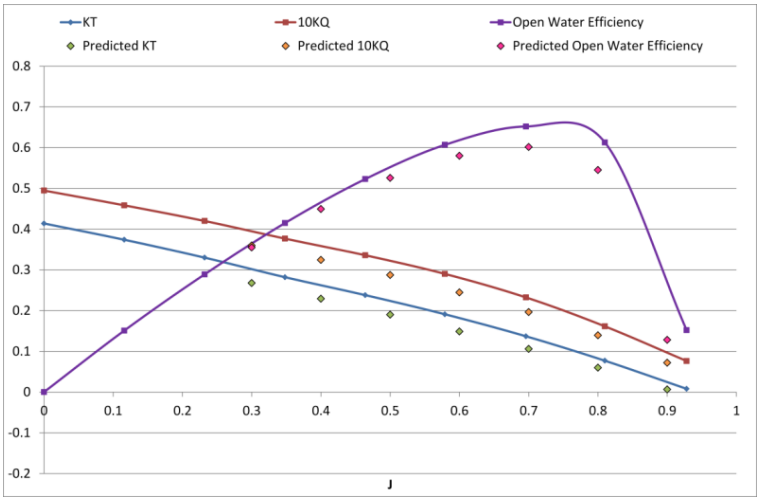

Figure 4: Comparison of experimental and predicted results for real propeller validation

As stated previously, whilst the geometry of the propeller in the tests and simulations matched, the additional shaft geometry was not included in the simulations. It is thought that these variations are the reason for the reduced accuracy in the CFD prediction. Variations in mesh configuration and time-step were tested to ascertain that they were not causing the inaccuracies and negligible differences in the results were observed. It is therefore felt that it is still justifiable to continue with this approach and this propeller.

4.2 PREDICTION (PARAMETRIC) STUDY

Full scale propeller open water simulations were carried out for the real propeller for each different fouling condition, as discussed in Table 2, at J = 0.3, J=0.5 and J=0.7. For these simulations, the propeller rotation speed, n, was kept constant at 1.412RPS / 84.72RPM. This propeller revolution speed was found to be the self-propulsion point in model scale tests. The inlet velocity, V_A, was varied in each case in order to achieve the required J value.

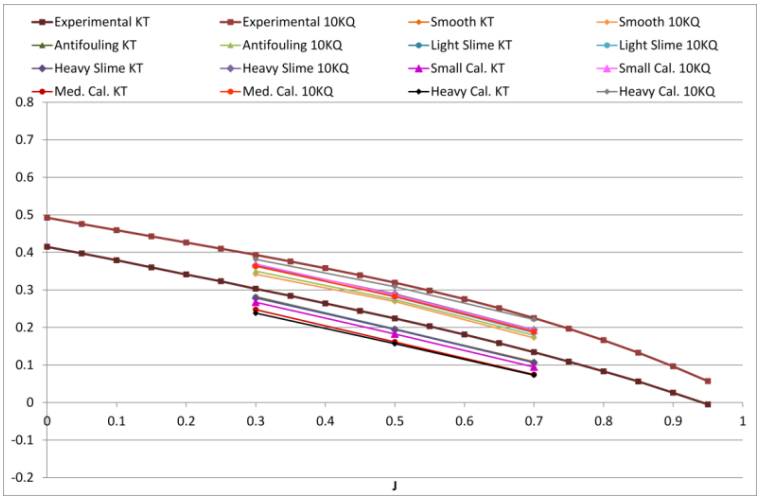

Figure 5: Comparison of K_T and $10K_Q$ with different levels of fouling at full scale

Figure 5 and Figure 6 present the results of the propeller performance predictions carried out using the outlined CFD approach, compared to the model scale open water test results scaled to full scale using the ITTC (2011a) approach. All the scaled model test results, for both open water and self-propulsion, are presented in (Aquo Consortium, 2014). It can be seen from the results that the thrust coefficient of the propeller is decreased by the presence of fouling, however the torque coefficient gradually increase with increased fouling roughness. This results in a gradual decrease in the propeller open water efficiency with increasing fouling roughness.

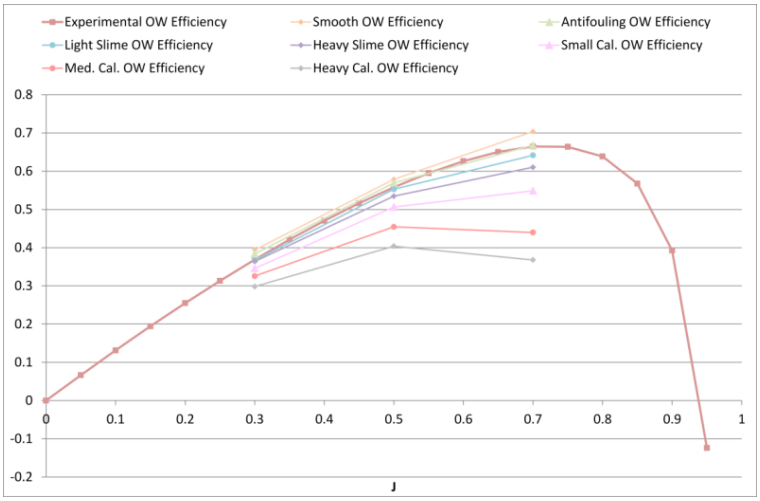

Figure 6: Comparison of propeller efficiency with different levels of fouling at full scale

Table 3 shows the decrease in efficiency for each level of fouling compared to the hydraulically smooth case, i.e. the validated propeller case, at each J value simulated, and also the difference averaged over the three J conditions. It can be seen in this table that in general the decrease in propeller efficiency is greater at higher J values than at lower ones. It can also be seen that as the propeller gets progressively more fouled, the decrease in efficiency increases steadily, which is also apparent in the graph.

Table 3: Changes in propeller efficiency at different levels of fouling.

Fouling Condition	Percentage Difference (%)		Average Percentage Difference (%)
Hydraulically Smooth Surface	J = 0.3	0	0
	J = 0.5	0	
	J = 0.7	0	
Typical As Applied Anti-Fouling Coating	J = 0.3	-2.61	-3.11
	J = 0.5	-1.62	
	J = 0.7	-5.10	
Deteriorated Coating or Light Slime	J = 0.3	-4.92	-6.09
	J = 0.5	-4.48	
	J = 0.7	-8.85	
Heavy Slime	J = 0.3	-7.69	-9.52
	J = 0.5	-7.61	
	J = 0.7	-13.28	
Small Calcareous Fouling or Weed	J = 0.3	-12.27	-15.60
	J = 0.5	-12.49	
	J = 0.7	-22.03	
Medium Calcareous Fouling	J = 0.3	-17.42	-25.46
	J = 0.5	-21.6	
	J = 0.7	-37.51	
Heavy Calcareous Fouling	J = 0.3	-24.39	-34.11
	J = 0.5	-30.20	
	J = 0.7	-47.76	

5 DISCUSSION AND CONCLUSIONS

In this paper, CFD approach for the prediction of propeller open water characteristics has been outlined and validated using a well-known bench-marking case. The same approach has then been applied to a model scale version of a real propeller, with the results again compared with model scale test result data, this time scaled to full scale using the ITTC approach. Although the agreement for the real propeller is less satisfactory, these

differences have been investigated and it appears that the variations in the geometry may account for the inaccuracy observed. This same propeller model has then been simulated in full scale, with different levels of fouling applied in the form of surface roughness functions.

It has been observed that the penalty for the presence of fouling on propeller open water efficiency can be significant, and would have a significant impact on the efficiency of a real vessel and hence its emissions. It should be noted that in this study, a uniform inflow was assumed into the propeller, which is not representative of a real case. In reality the propeller would not only be operating in the wake of a ship hull but also most likely a fouled ship hull, further changing the operational conditions away from the design point by modifying the wake, and hence further impacting on the propeller efficiency. Using an approach such as that demonstrated in this paper, industry could investigate the impact of fouling on their own propeller designs, and could hence use the efficiency changes predicted within a decision-making framework to schedule when it would be economically beneficial to drydock the vessel or at least clean the propeller. They could also be used to investigate the advantages of applying anti-fouling coatings to the propeller as well as the hull.

It can also be observed from the full scale comparison that despite the variations in the predicted KT and 10KQ, the overall efficiencies are close to the scaled model test results. However, it should be noted that the efficiency results which most closely match the tests are those with a surface roughness equivalent to anti-fouling coating rather than a hydraulically smooth surface. The hydraulically smooth results slightly over-predict the propeller open water efficiency. This is natural as the surface of the model propeller is also extremely unlikely to be hydraulically smooth. This is an aspect which should be considered by users of CFD in future studies for the prediction of propeller performance and comparison of numerical and experimental results; in order to obtain the best agreement, a small amount of propeller surface roughness may need to be included in the simulation.

It can be concluded that the approach developed within this paper is suitable both for the prediction of propeller open water performance in general, but also for the prediction of the impact of roughness arising from marine fouling. As with any CFD work, care must be taken in applying an approach to a case where no direct validation data is available, and sources of error and inaccuracy must be appreciated when using any results generated.

ACKNOWLEDGEMENTS

The authors gratefully acknowledge the partners of the EU-funded FP7 Project AQUO (Achieve QUieter Oceans by shipping noise footprint reduction, Project Reference: 314227 under FP7-SST-2012-RTD-1), and in particular SSPA, TSI, University of Genoa and CEHIPAR for providing full and model scale data for the case study vessel.

The authors gratefully acknowledge that the research presented in this paper was partially generated as part of the EU funded FP7 project FOUL-X-SPEL (Environmentally Friendly Antifouling Technology to Optimise the Energy Efficiency of Ships, Project number 285552, FP7-SST-2011-RTD-1).

Results were obtained using the EPSRC funded ARCHIE-WeSt High Performance Computer (www.archie-west.ac.uk). EPSRC grant no. EP/K000586/1.

REFERENCES

Apsley, D. (2007). CFD calculation of turbulent flow with arbitrary wall roughness. *Flow, Turbulence and Combustion,* 78**,** 153-175.

Aquo Consortium. (2012). *RE: Achieve QUieter Oceans by Shipping Noise Footprint Reduction.*

Aquo Consortium (2014). D2.5: Propeller noise experiments in model scale.

Aquo Consortium (2015a). D2.3: Predictive theoretical models for propeller URN.

Aquo Consortium (2015b). D5.5: Impact of solutions on fuel efficency.

ARCHIE-WeSt. *ESPRC funded ARCHIE-WeSt High Peformance Computer* [Online]. Available: http://www.archie-west.ac.uk/.

Arikan, Y., Drogul, A. & Celik, F. (2012). Performance analysis and investigation of the slipstream flow of podded propellers. Brodo Gradnja. 226-233.

Aupoix, B. (2007). A general strategy to extend turbulence models to rough surfaces: application to Smith's k-L model. *Journal of Fluids Engineering,* 129**,** 1245-1254.

Bertram, V. (2011). *Practical ship hydrodynamics (second edition)*, Butterworth-Heinemann.

Castro, A. M., Carrica, P. M. & Stern, F. (2011). Full scale self-propulsion computations using discretized propeller for the KRISO container ship KCS. *Computers & Fluids,* 51**,** 35-47.

CD-ADAPCO (2014). User Guide STAR-CCM+, Version 9.02.011.

Cebeci, T. & Bradshaw, P. (1977). *Momentum transfer in boundary layers*, Hemisphere Publishing Corporation/McGraw-Hill.

Da-Qing, L. (2002). Validation of RANS predictions of open water performance of a highly skewed propeller with experiments. Conference of Global Chinese Scholars on Hydrodynamics.

Demirel, Y. K., Khorasanchi, M., Turan, O. & Incecik, A. (2013). A parametric study: Hull roughness effect on ship frictional resistance. Proceedings of the International Conference on Marine Coatings, London, UK.

Demirel, Y. K., Khorasanchi, M., Turan, O. & Incecik, A. (2014a). CFD approach to resistance prediciton as a function of roughnes. Proceedings of Transport Research Arena Conference 2014, Paris La Defense, France.

Demirel, Y. K., Khorasanchi, M., Turan, O., Incecik, A. & Schultz, M. P. (2014b). A CFD model for the frictional resistance prediction of antifouling coatings. *Ocean Engineering,* 89**,** 21-31.

Demirel, Y. K., Turan, O. & Incecik, A. (2015). A CFD model for the prediction of the effect of biofouling on frictional resistance. *Applied Ocean Research,* under review.

Eça, L. & Hoekstra, M. (2011). Numerical aspects of including wall roughness effects in the SST k–ω eddy-viscosity turbulence model. *Computers & Fluids,* 40**,** 299-314.

Fang, I., Cheng, F., Incecik, A. & Carnie, P. (2013). Global Marine Trends 2030. London.

Ferziger, J. H. & Peric, M. (2002). *Computational Methods for Fluid Dynamics*, Springer.

FOUL-X-SPEL. (2011). *FOUL-X-SPEL : Environmentally friendly antifouling technology to optimise the energy efficiency of ships* [Online]. http://www.foulxspel-antifouling.com/.

Granville, P. S. (1958). The frictional resistance and turbulent boundary layer of rough surfaces. *Journal of Ship Research,* 2**,** 52-74.

Granville, P. S. (1978). Similarity-law characterization methods for arbitrary hydrodynamic roughnesses. *Final Report Naval Ship Research and Development Center, Bethesda, MD. Ship Performance Dept.,* 1.

Grigson, C. (1985). The drag at ship scale of planes having any quality of roughness. *Journal of Ship Research,* 29**,** 94-104.

Hansen, H. R. & Dinham-Peren, T. (2014). EEDI challenges in the design of large slow-speed ships. London,UK.

Hansen, H. R., Dinham-Peren, T. & Nojiri, T. (2011). Model and full scale evaluation of a 'Propeller Boss Cap Fins' device fitted to an afromax tanker. Symposium on Marine.

Haslbeck, E. G. & Bohlander, G. (1992). Microbial biofilm effects on drag-lab and field. *1992 Ship Production Symposium Proceedings, SNAME.*

Hsin, C.-Y., Lin, B. H. & Lin, C.-C. (2009). The optimum design of a propeller energy saving device by computational fluid dynamics. Computational Fluid Dynamics.

Hundley, L. & Tate, C. (1980). Hull-fouling studies and ship powering trial results on seven FF 1052 class ships. *D W Taylor Naval Ship Research and Development Center Report # DTNSRDC-80/027. 111 p.*

IMO. (2009a). MEPC 59/4/15, Prevention of air pollution from ships, Energy Efficiency Operational Indicator (EEOI)

IMO (2009b). Second IMO GHG Study 2009. London,UK.

IMO. (2014). Annex 5, Resolution MEPC.245(66), 2014 Guidelines on the method of calculation of the attained Energy Efficiency Design Index (EEDI) for new ships.

ITTC (1990). Report of the Powering Performance Committee. Proceedings of the 19th ITTC.

ITTC. (2011). Specialist Committee on Surface Treatment – Final report and recommendations to the 26th ITTC. Proceedings of 26th ITTC – Volume II

Jiménez, J. (2004). Turbulent flows over rough walls. *Annual Review of Fluid Mechanics,* 36**,** 173-196.

Kawamura, T., Ouchi, K. & Nojiri, T. (2012). Model and full scale CFD analysis of Propeller Boss Cap Fins (PBCF). J MAR Sci Technol, Tasmania, Australua. 469-480.

Kellet, P., Turan, O. & Incecik, A. (2013). A study of numerical ship underwater noise predictiion Ocean Engineering

Khor, Y. S. & Xiao, Q. (2011). CFD simulations of the effects of fouling and antifouling. *Ocean Engineering,* 38**,** 1065-1079.

Krogstad, P.-A. (1991). Modification of the van Driest damping function to include the effects of surface roughness. *AIAA Journal,* 29**,** 888-894.

Mizzi, K., Demirel, Y. K., Banks, C., Turan, O. & Kaklis, P. (2014). PBCF design optimisation and propulsion efficiency impact. RINA International Conference on Influence of EEDI on Ship Design, London.

Nakisa, M., Abbasi, M. J. & Amini, A. M. (2010). Assessment of marine propeller hydrodynamic performance in open water via CFD. The International Conference on Marine Technology, Bangladesh. Proceedings of MARTEC 2010, 35-44.

Naval Ships' Technical Manual (2002). Waterborne underwater hull cleaning of navy ships. S9086-CQ-STM-010/CH-081R5. . *Naval Sea Systems Command*.

Nikuradse, J. (1933). *Laws of flow in rough pipes*, NACA Technical Memorandum 1292.

Patel, V. C. (1998). Perspective: Flow at high reynolds number and over rough surfaces—Achilles heel of CFD. *Journal of Fluids Engineering,* 120**,** 434-444.

Patience, G. & Atlar, M. (1998). An investigation into effective boss cap designs to eliminate propeller hub vortex cavitation. Proceedings of the 7th International Symposium on Practical Design of Ships and Mobile Units The Hague

Queutey, P., Guilmineau, E., Deng, G. B. & Salvatore, F. (2013). A comparison between full RANSE and coupled RANSE-BEM approaches in ship propulsion performance prediction Proceedings of the ASME 2013 32nd International Conference on Ocean, Offshore and Arctic Engineering Nantes, France.

Schuiling, B. (2013). The design and numerical demonstration of a new energy saving device. 16th Numerical Towing Tank Symposium. 141-146.

Schultz, M. P. (2004). Frictional resistance of antifouling coating systems. *Journal of Fluids Engineering,* 126**,** 1039-1047.

Schultz, M. P. (2007). Effects of coating roughness and biofouling on ship resistance and powering. *Biofouling,* 23**,** 331-341.

Schultz, M. P. & Flack, K. (2007). The rough-wall turbulent boundary layer from the hydraulically smooth to the fully rough regime. *Journal of Fluid Mechanics,* 580**,** 381-405.

Shockling, M. A., Allen, J. J. & Smits, A. J. (2006). Roughness effects in turbulent pipe flow. *Journal of Fluid Mechanics,* 564**,** 267-285.

Suga, K., Craft, T. J. & Iacovides, H. (2006). An analytical wall-function for turbulent flows and heat transfer over rough walls. *International Journal of Heat and Fluid Flow,* 27**,** 852-866.

SVA Hydrodynamic Solutions. SVA.

UNFCCC. *Kyoto Protocol* [Online]. http://unfccc.int/kyoto_protocol/items/2830.php. [Accessed 04 / 05 / 2015].

Vladimir, K., Jiaying, S. & Henning, H. K. (2009). CFD investigation in scale effect on propellers with different magnitude of skew in turbulent flow. First International Symposium on Marine Propulsors, Norway.